A&A 371, 1012–1017 (2001)
DOI: 10.1051/0004-6361:20010451

Astronomy & Astrophysics

Magnetic field structure in the outer OH maser envelope of VX Sagittarii

M. Szymczak[1], R. J. Cohen[2], and A. M. S. Richards[2]

[1] Toruń Centre for Astronomy, Nicolaus Copernicus University, ul. Gagarina 11, 87100 Toruń, Poland
[2] Jodrell Bank Observatory, University of Manchester, Macclesfield, Cheshire, SK11 9DL, UK

Received 29 January 2001 / Accepted 15 March 2001

Abstract. The OH 1612 MHz maser transition from the supergiant star VX Sgr has been imaged in all Stokes parameters using MERLIN. Numerous elliptically polarised components are distributed in a roughly symmetric envelope of a size similar to that measured in total maser intensity. The polarisation vectors are generally tangential to the circumstellar envelope, indicating a globally ordered magnetic field at the distance of about 1400 au from the supergiant. It is suggested that a predominance of projected radial magnetic lines and a displacement between the red- and blue-shifted parts of the envelope can be explained with a dipole field tilted at 20−30° to the line of sight.

Key words. masers – polarisation – stars: magnetic fields – stars: circumstellar matter – stars: supergiants – stars: individual: VX Sgr

1. Introduction

Circular polarisation is a distinctive characteristic of OH masers around late-type supergiant stars. Observations at high spectral resolution revealed several polarised features with line widths as small as 0.1 km s^{-1} in the OH 1612 MHz spectra of four supergiants including VX Sgr (Cohen et al. 1987). The presence of circular polarisation was itself evidence for Zeeman splitting (Deguchi & Watson 1986) and, despite difficulties in identifying classical Zeeman patterns, provided a direct estimate of the strength and direction of the magnetic field. High angular resolution data enabled more reliable identification of Zeeman pairs in two supergiants; IRC+10420 (Kemball 1992) and VX Sgr (Szymczak & Cohen 1997). In the latter object, the magnetic field strength was estimated to be ∼1 mG at a distance of about 1400 au from the star, directed towards the observer (Szymczak & Cohen 1997; Trigilio et al. 1998). The spatial distribution of the 1612 MHz emission in VX Sgr observed with the VLA (Zell & Fix 1996) and MERLIN (Szymczak & Cohen 1997) indicates a remarkable segregation between components of opposite circular polarisation, suggesting a globally ordered magnetic field.

It has been suggested that the axi-symmetric geometry of the 1612 MHz maser envelope of VX Sgr, reported first by Chapman & Cohen (1986), is a characteristic of radiation driven mass loss in circumstances where the effect of the circumstellar magnetic field cannot be neglected (Szymczak & Cohen 1997). There is as yet no clear mechanism to explain the impact of the magnetic field on the stellar wind in the outer parts of circumstellar envelopes. The effect of the magnetic field on charged dust particles was postulated by Chapman & Cohen (1986). On the other hand, the presence of free electrons in circumstellar material (Szymczak et al. 1998) would freeze the magnetic field into the outflowing gas. The magnetic field also affects the OH maser properties through the magnetic beaming phenomenon described by Gray & Field (1995).

Linearly polarised OH emission from circumstellar envelopes has rarely been studied (Cohen 1989). Weak and narrow linearly polarised OH mainline masers (at 1665 and 1667 MHz) are seen at the most blue-shifted velocities in Mira-type stars (Szymczak et al. 1998). There are no published reports of searches for linear polarisation of OH emission towards VX Sgr. However, to understand the polarisation mechanisms of OH masers and the possible role of the magnetic field in the dynamics of the circumstellar envelope, full polarisation data at high angular resolution are needed. In this paper we report the first results of the polarisation structure of VX Sgr at 1612 MHz observed with MERLIN in full polarisation mode and consider the morphology of inferred circumstellar magnetic field in the outer OH maser envelope.

Send offprint requests to: M. Szymczak,
e-mail: msz@astro.uni.torun.pl

2. Observations and data reduction

The OH 1612 MHz maser transition was observed on 1999 April 24 using all seven telescopes of MERLIN, giving a minimum fringe spacing of ∼0.15 arcsec. A spectral bandwidth of 250 kHz was used, divided into 256 channels. This gave a velocity coverage of 46 km s^{-1} and a channel spacing of 0.18 km s^{-1}. In order to observe the whole velocity range of emission from VX Sgr, two bands centred on LSR velocities ($V_{\rm LSR}$) of −10 and +20 km s^{-1} were observed alternately, switching between them every 5 min. The target was tracked for 6 h. The left and right circularly polarised signals (LHC, RHC) from each pair of telescopes were correlated in full cross-polarisation mode, so that all Stokes parameters were obtained.

The initial data editing and correcting for gain-elevation effects was carried out using local programs for MERLIN data reduction. All further data processing were performed within the AIPS package in several steps (see Szymczak et al. 1998 for details) taking special care to calibrate the polarisation. The flux scale was derived using 3C286 (Baars et al. 1977) and the strong continuum source 3C84 was used to calibrate the bandpass. The flux of 3C84 was found to be 25.3 ± 1.4 Jy, giving a total flux scale error of ∼7%. The point continuum source 2134 + 004 was tracked for 20 min at three hour angles to correct for parallactic angle rotation and instrumental feed leakage, and 3C286 was used to calibrate the polarisation angle, with a $\sigma_{\rm rms} < 2^\circ$. These corrections were then applied to the VX Sgr data.

For both parts of the 1612 MHz spectrum, the brightest channels were examined to find channels containing point-like emission, positionally coincident in LHC and RHC polarisations. Suitable channels were identified at –13.8 and 24.9 km s^{-1} in the blue- and red-shifted data sets, respectively. (The terms blue-shifted and red-shifted are used to describe velocities relative to the stellar velocity of 5.5 km s^{-1}.) Phase only self-calibration was then carried out on these two reference channels using point models, and the solutions applied to all spectral channels of the VX Sgr data. Map cubes in all Stokes parameters were made and cleaned with 1000 cycles per channel using a 0.4 arcsec circular Gaussian restoring beam. The rms noise level in a line-free channel of I Stokes was ∼15 mJy beam^{-1}, corresponding to a brightness temperature of $4\,10^4$ K. The positions of the maser components were measured with a typical accuracy of 0.05 arcsec by fitting two-dimensional Gaussian components. The emission at 3.6 km s^{-1} appeared in both the blue- and red-shifted data sets and was used to align the data cubes spatially. The measured fluxes of this component in both data cubes agree to within the flux scale errors.

3. Results

The spectra for individual Stokes parameters and the percentages of polarisation are shown in Fig. 1. The fractions of circular and linear polarisation are defined as $m_{\rm c} = V/I$ and $m_{\rm l} = \sqrt{Q^2+U^2}/I$, respectively. At outermost velocities the linearly polarised intensity ($\sqrt{Q^2+U^2}$) is about one order of magnitude weaker than the total intensity. There are only a few linearly polarised features which have flux density greater than 2 Jy. Nevertheless, the polarised intensity $\sqrt{Q^2+U^2}$ profile, like the Stokes V profile, reveals several narrow features. The percentage of linear polarisation is usually lower than 10% at the outermost velocities and slightly increases towards the stellar velocity exceeding 20% for a few features.

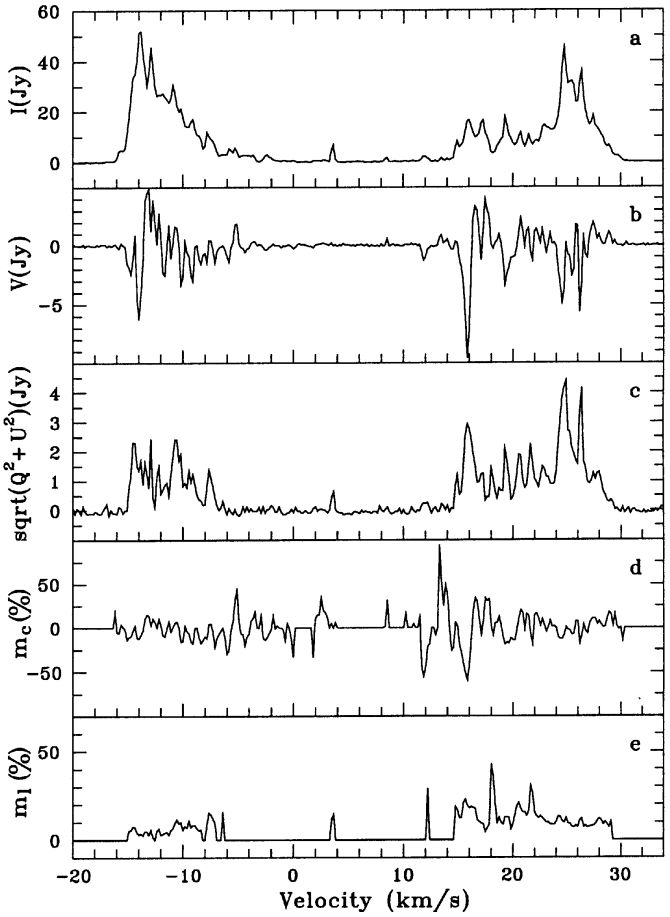

Fig. 1. MERLIN spectra of the polarisation of OH 1612 MHz maser emission from VX Sgr. The plots show **a)** Stokes I (total flux density), **b)** Stokes V (circularly polarised flux density), **c)** Stokes $(Q^2+U^2)^{1/2}$ (linearly polarised flux density), **d)** $m_{\rm c}$ (percentage circular polarisation) and **e)** $m_{\rm l}$ (percentage linear polarisation)

The relative positions of linearly polarised maser components are plotted in Fig. 2. The orientation of the linear polarisation vectors defines the plane of the electric field vectors and their lengths are proportional to the linearly polarised intensity $\sqrt{Q^2+U^2}$. The origin of this map is the position of central star inferred from a symmetrical shell model applied to the present Stokes I data set as described in Szymczak & Cohen (1997). This map shows a clearly defined broad ring of emission which follows the envelope of roughly symmetric shape seen in the Stokes I parameter. The polarisation vectors are generally

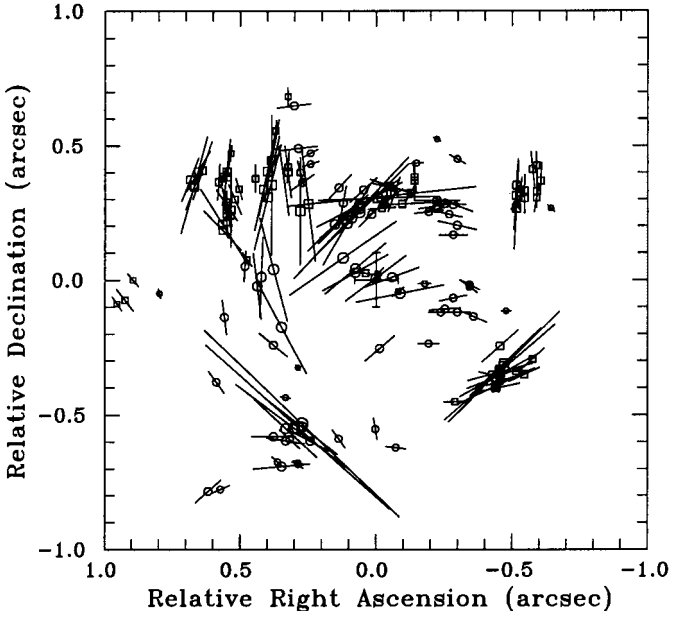

Fig. 2. Relative positions of the OH 1612 MHz linearly polarised maser components of VX Sgr. The bars represent the plane of the electric field vector and have lengths proportional to the peak brightness of linearly polarised components, where 0.1 arcsec $\equiv$ 0.41 Jy beam^{-1}. The circles and squares represent the blue- and red-shifted components, respectively. The size of each symbol is proportional to the logarithm of the linearly polarised intensity. The filled circle and error bars at the diagram origin denote the inferred stellar position (see text) and its uncertainty, respectively

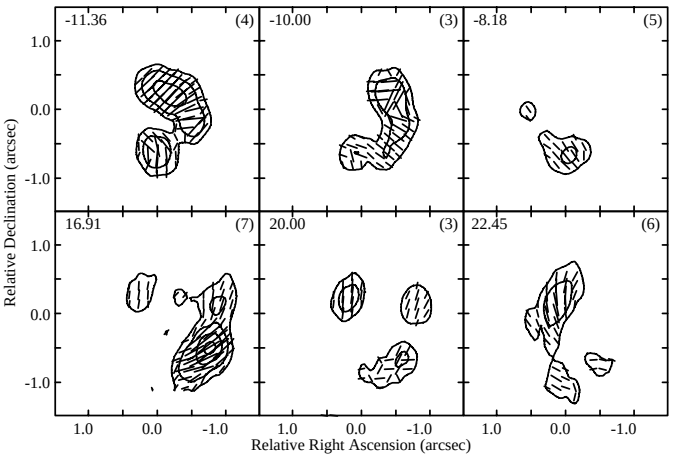

Fig. 3. Selected linear polarisation ($\sqrt{Q^2+U^2}$) maps of the 1612 MHz maser emission of VX Sgr. Contour levels are $(-1,\ 1,\ 2,\ 4,\ 6)\times 100$ mJy beam^{-1}. Bars show the orientations of the electric vectors and have lengths proportional to the linearly polarised intensities, where 0.1 arcsec $\equiv$ 0.11 Jy. The central LSR velocity (km s^{-1}) of each map is indicated in the upper left-hand corner. The number of contiguous channels averaged is given in the upper right-hand corner

tangential to the circumstellar envelope, that is, perpendicular to the radial direction from the star.

In addition to the strong components plotted in Fig. 2 there are also fainter regions of linearly polarised emission. Selected averaged channel maps of Stokes $\sqrt{Q^2+U^2}$ are shown in Fig. 3. The orientations of the polarisation vectors in the regions of weak and extended emission commonly follow the trend seen in Fig. 2. However in some channel maps the orientation of the polarisation vectors is clearly structured but at orientations very different from tangential (panels at -11.36 and -10 km s^{-1} in Fig. 3). This could be due to a projection effect or complex structures in the circumstellar magnetic field.

To check more quantitatively the orientation of polarisation vectors in the envelope, we defined the deviation of the polarisation angle from the radial direction, relatively to the stellar position, as $\mathrm{PA_c}-\mathrm{PA_p}$, where $\mathrm{PA_c}$ is the position angle of a maser component around the plane of the sky and $\mathrm{PA_p}$ is the position angle of the polarisation vector. Figures 4 and 5 show this deviation as a function of $\mathrm{PA_c}$ and velocity, respectively. 104 out of 159 components (65%) have polarisation vectors orthogonal, within $\pm 30°$, to the radial direction, whereas only 17% of components are parallel within $\pm 30°$. This trend is even stronger when the brightness of linearly polarised components is considered: components with $\mathrm{PA_p}$ "parallel" to $\mathrm{PA_c}$ are usually weaker than 0.4 Jy beam^{-1} (Fig. 4).

A significant departure from this trend is observed in the range of $\mathrm{PA_c}$ from 30 to 100°. 12 out of 30 components with linearly polarised brightness exceeding 0.8 Jy beam^{-1} are not orthogonal to the radial direction (within $\pm 30°$). All these 12 components are seen at $V_{\mathrm{LSR}} > 23.8$ km s^{-1} (Figs. 3 and 5) and possibly mark a site of complex magnetic field structure. The $\mathrm{PA_c}-\mathrm{PA_p}$ of red-shifted components, in contrast to that of blue-shifted ones, exhibit a weak systematic change with the radial velocity (Fig. 5). There are 7 red-shifted components with fractional linear polarisation higher than 50%; all of them are located in the north-eastern cluster of the envelope. Neglecting these strongly polarised components, possibly associated with a local field structure or caused by a projection effect, we still notice that the mean angle $\mathrm{PA_c}-\mathrm{PA_p}$ is 90° for $V_{\mathrm{LSR}} < 20$ km s^{-1}, but about 120° for $V_{\mathrm{LSR}} > 20$ km s^{-1}.

Figure 6 shows the percentage of linear polarisation versus the percentage of circular polarisation for all 159 components with the peak brightness higher than 150 mJy beam^{-1} in Stokes $\sqrt{Q^2+U^2}$ and V. The percentage of polarisation is shown as zero if the linearly or circularly polarised flux densities are less than the noise level. There are only 19 components (12%) with $m_{\mathrm{l}} > 30\%$ and most of them are red-shifted. Strong circular polarisation ($|m_{\mathrm{c}}| > 65\%$) is visible only for blue-shifted components. Figure 6 clearly illustrates that all components are elliptically polarised and only 5 components are 100% polarised. There are 8 components with $|m_{\mathrm{c}}| < 35\%$, but with high linear polarisation ($m_{\mathrm{l}} > 50\%$). 7 out of 8 components have $-20° < \mathrm{PA_p} < 20°$ and are located in the northern side of the envelope. If these are interpreted as π components then the orientation of the magnetic field agrees very well with an overall picture of radial field geometry. We notice, however, that in the same region and

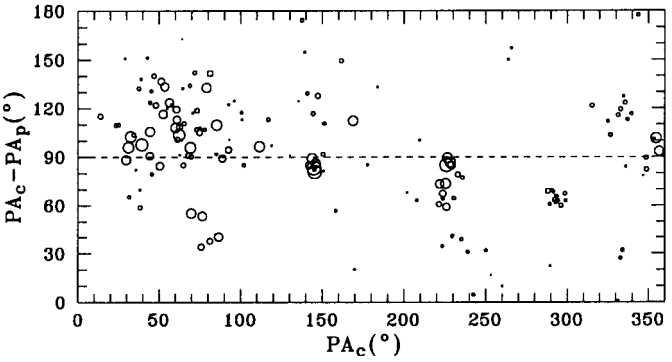

Fig. 4. Deviation of polarisation angle from the radial direction ($PA_c - PA_p$) versus the position angle of maser component around the plane of the sky (PA_c). The size of each circle is proportional to the logarithm of the brightness of linearly polarised components (the largest circle corresponds to 4.13 Jy beam^{-1})

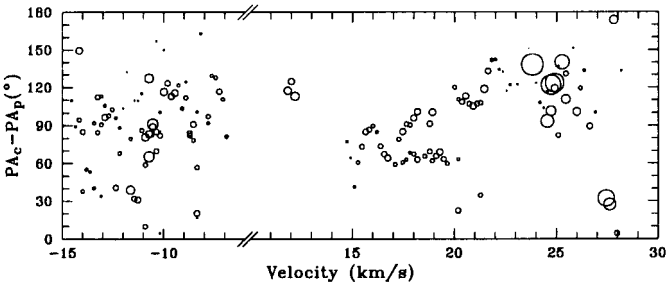

Fig. 5. Deviation of polarisation angle from the radial direction ($PA_c - PA_p$) versus the radial velocity. The size of each circle is proportional to the fractional linear polarisation (the largest circle means 88%)

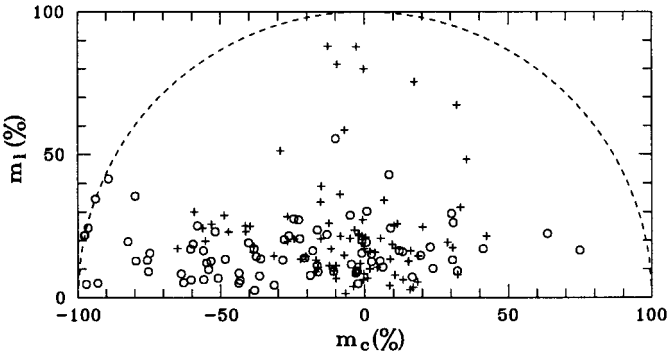

Fig. 6. Percentage of linear versus circular polarisation of 1612 MHz OH maser spots in VX Sgr. Circles and crosses indicate the blue-shifted and red-shifted emission, respectively. Completely polarised components lie on the dashed line

range of PA_p there are many more components with low m_l which hardly can be interpreted as π components.

To determine properly the magnetic field direction from the orientations of polarisation vectors in a given portion of the envelope one needs to know whether the linearly polarised components are σ or π components of the Zeeman pattern. If the magnetic field is perpendicular to the line of sight the σ components are linearly polarised perpendicular to the field, whereas the π components are linearly polarised parallel to the field. We searched for groups of maser components of circular and linear polarisation that coincide in the sky to within measurement accuracy. In some places, likely Zeeman pairs with LHC and RHC components but without linearly polarised components were found. More details on the pairs of σ components of opposite circular polarisation and their temporal behaviour will appear in a separate paper.

4. Discussion

The major result from MERLIN observations presented in this paper is that the morphology of the polarisation vectors of the elliptically polarised components shows a large scale order. The OH 1612 MHz maser emission from VX Sgr possibly traces the spatial orientation of the magnetic field in the outer parts of the circumstellar envelope. However, there is an ambiguity about the inferred field direction, depending on whether the elliptical polarisation represents π or σ components. We assume that most elliptically polarised components in our data are σ components. This assumption appears to be consistent with observations of OH 1665 MHz masers in star forming regions. Garcia-Barreto et al. (1988) found no features in W3(OH) which might be interpreted as π components. Observations of G35.2−0.74N have shown that all Zeeman pairs identified contain σ components only (Hutawarakorn & Cohen 1999). Theoretical studies of polarised maser emission predict a dominance of σ components in a wide range of values of the ratio of the Zeeman splitting to the Doppler line width (x_B) and the degree of maser saturation (Elitzur 1996). Suppression of π components is expected especially for $x_B > 0.1$ and saturated emission, conditions usually fulfilled in OH 1612 maser regions. It is therefore plausible that in VX Sgr we generally observed σ components, in which case the projected circumstellar magnetic field has a predominantly radial geometry.

The plane of elliptical polarisation could change due to internal Faraday rotation and the apparent polarisation vectors would not then be orthogonal to the projected direction of the magnetic field. The OH 1612 MHz envelope of VX Sgr is asymmetric and moreover the emission at the extreme red- and blue-shifted velocities does not coincide in the plane of the sky (Chapman & Cohen 1986; Szymczak & Cohen 1997). Therefore, the red-shifted linearly polarised emission possibly propagates along the paths where the electron density is too low to strongly rotate the plane of linear polarisation. Indeed, PA_c for the red-shifted emission from VX Sgr differs by 30−50° from the PA_c of the rest of the emission (Fig. 5). If this is interpreted as Faraday rotation then for a magnetic field of 1.1 ± 0.4 mG inferred from a Zeeman splitting (Szymczak & Cohen 1997) and for the assumed maser gain length of 10^{16} cm the required electron density is 24 cm^{-3}. We note, however, that the above value of magnetic field was evaluated with implicit assumption that $x_B > 1$. Following Elitzur's (1996) theory for $x_B < 1$ the magnetic field strength re-evaluated from that Zeeman pair is only

0.3 mG for angle 45° from the direction of the magnetic field. Nevertheless, for the model of the 1612 MHz maser (Elitzur et al. 1976) with a gas density of $10^6\,\mathrm{cm}^{-3}$ and the kinetic temperature 100 K, a magnetic field of 0.3 mG provides a magnetic pressure comparable to that caused by thermal gas motions, so that it may has non-negligible consequences on the outflow dynamics.

The orientation of the polarisation vectors might be affected by external Faraday rotation in the interstellar medium. VX Sgr is at $l = 8\overset{\circ}{.}34$ and $b = -1\overset{\circ}{.}00$, close to the direction of the Galactic centre. The local strength of the longitudinal magnetic field is about 1.3 μG (Rand & Kulkarni 1989) and the average number density of the interstellar medium is $0.5\,\mathrm{cm}^{-3}$ with a fractional ionisation of 10^{-4} (Garcia-Barreto et al. 1988). For a distance of 1.7 kpc to VX Sgr, this would only rotate the polarisation vectors by about $0\overset{\circ}{.}2$. It is therefore unlikely that the observed polarisation vectors are strongly influenced by the interstellar medium. An electron density higher than $0.05\,\mathrm{cm}^{-3}$, implying a fractional ionisation two orders of magnitude higher, would be required to significantly change the plane of the polarisation vectors in the manner observed towards more distant pulsars near the Galactic centre (Clegg et al. 1992).

The average distance of the 1612 MHz masers from VX Sgr is about 1400 au. The OH mainline and H_2O masers occur much closer to the star at distances of 200−400 au (Chapman & Cohen 1986; Bowers et al. 1993). The SiO 43 GHz masers are located about 30 au from the star (Greenhill et al. 1995). Zeeman splitting observed in OH mainline masers (Chapman & Cohen 1986) implies the magnetic field strength of about 2 mG. (In this case $x_\mathrm{B} \approx 1$, so any correction for propagation effects will be small (Elitzur 1996; 1998).) Although the magnetic field near the stellar surface can be uncertain as the SiO maser polarisation is not strongly dependent on field strength (Nedoluha & Watson 1994), an estimate by Elitzur (1996) provides a value of about 10 G at distance of 30 au from the star. The field strength re-evaluated above from the 1612 MHz data, projected back to the SiO maser envelope, accordingly to a dipole law (r^{-3}), yields a field of about 35 G. This value agrees well with Elitzur's estimate considering that only the largest Zeeman splitting is used. Therefore, a dipole field is plausible.

The morphology of linear polarisation vectors implies a predominantly radial magnetic field in the outer envelope of VX Sgr. This picture is consistent with a dipole field viewed end-on. If the dipole is tilted by about 20 or 30° to the line of sight we will still see a projected radial field pattern in the linear polarisation and at the same time account for the displacement between regions of high circular polarisation on the near and far sides of the OH 1612 MHz shell (Zell & Fix 1996; Szymczak & Cohen 1997). Detailed modelling of the magnetic field configuration will need to take propagation effects into account and is postponed to a later paper. The following observational evidence will need to be explained: (i) The linear polarisation vectors of the 1612 MHz emission are predominantly tangential to the circumstellar envelope, implying a predominantly radial magnetic field. (ii) However, the field in the red-shifted NE section of the envelope departs from the generally radial field. (iii) The magnetic field is sampled only in those regions where the propagation of polarised maser emission is strongly favoured. (iv) Ordered polarisation is seen in the brightest emission: however, some regions of weaker emission do not always follow the same polarisation trends seen in the strongest emission. (v) Circular polarisation of 1612 MHz emission indicates a magnetic axis projected at position angle $210 \pm 20°$ on the plane of the sky, with the field direction towards us (Szymczak & Cohen 1997; Trigilio et al. 1998). (vi) OH mainline emission at 1667 MHz, which samples a region five times closer to the star than 1612 MHz emission, is consistent with the same magnetic axis (Richards et al. 2000).

5. Conclusions

We have obtained MERLIN images of the OH 1612 MHz maser emission from VX Sgr with full polarisation information. The linear polarisation vectors are predominantly tangential to the circumstellar envelope. This implies that the magnetic field geometry is predominantly radial (since we are most likely observing σ components of the Zeeman splitting). However the polarisation vectors in regions of weak and extended emission do not always follow the trend observed in the brightest components, and there is one sector of the OH 1612 MHz envelope (NE red-shifted) where strong deviations are observed from the radial field geometry. The observational evidence is broadly consistent with a dipole magnetic field not quite end-on, but tilted to the line of sight by 20 or 30°. Detailed modelling is needed to confirm the magnetic field configuration more accurately and to determine the nature of the field distortions apparent in the red-shifted NE sector of the envelope. Such modelling could also incorporate magnetic field information obtained from other masers, such as OH mainlines at 1665 and 1667 MHz and SiO lines near 43 and 86 GHz, which originate nearer to the star, down to distances of only a few stellar radii.

Acknowledgements. We thank the MERLIN staff for help with the observations. MERLIN is a national facility operated by the University of Manchester at Jodrell Bank Observatory on behalf of PPARC.

References

Baars, J. W. M., Genzel, R., Pauliny-Toth, I. I. K., & Witzel, A. 1977, A&A, 61, 99

Bowers, P. F., Claussen, M. J., & Johnston, K. J. 1993, AJ, 105, 284

Chapman, J. M., & Cohen, R. J. 1986, MNRAS, 220, 513

Clegg, A. W., Cordes, J. M., Simonetti, J. H., & Kulkarni, S. R. 1992, ApJ, 386, 143

Cohen, R. J. 1989, RPPh, 52, 881

Cohen, R. J., Downs, G., Emerson, R., et al. 1987, MNRAS, 225, 491
Deguchi, S., & Watson, W. D. 1986, ApJ, 300, L15
Elitzur, M. 1996, ApJ, 457, 415
Elitzur, M. 1998, ApJ, 504, 390
Elitzur, M., Goldreich, P., & Scoville, N. 1976, ApJ, 205, 384
Garcia-Barreto, J. A., Burke, B. F., Reid, M. J., et al. 1988, ApJ, 326, 954
Gray, M. D., & Field, D. 1995, A&A, 298, 243
Greenhill, L. J., Colomer, F., Moran, J. M., et al. 1995, ApJ, 449, 365
Hutawarakorn, B., & Cohen, R. J. 1999, MNRAS, 303, 845
Kemball, A. J. 1992, Ph.D. Thesis, Rhodes Univ., Grahamstown
Nedoluha, G. E., & Watson, W. D. 1994, ApJ, 423, 394
Rand, R. J., & Kulkarni, S. R. 1989, ApJ, 343, 760
Richards, A. M. S., Cohen, R. J., Murakawa, K., et al. 2000, OH masers and the structure of Mira/Red Supergiant winds, in Proceedings of the 5th European VLBI Network Symposium, ed. J. E. Conway., A. G. Polatidis, R. S. Booth, & Y. Pihlström, OSO, 185
Szymczak, M., & Cohen, R. J. 1997, MNRAS, 288, 945
Szymczak, M., Cohen, R. J., & Richards, A. M. S. 1998, MNRAS, 297, 1151
Trigilio, C., Umana, G., & Cohen, R. J. 1998, MNRAS, 297, 497
Zell, P. J., & Fix, J. D. 1996, AJ, 112, 252